Employing typicality in optimal control theory: Addressing large Hilbert spaces

Aviv Aroch* and Ronnie Kosloff
The Institute of Chemistry, The Hebrew University of Jerusalem, Jerusalem 9190401, Israel

Shimshon Kallush
Sciences Department, Holon Academic Institute of Technology, 52 Golomb Street, Holon 58102, Israel

(Received 6 September 2022; accepted 3 January 2023; published 6 February 2023)

Controlling the dynamics of quantum systems is a crucial task in quantum science and technology. Obtaining the driving field that transforms the quantum systems into its objective is a typical control task. This task is hard, scaling unfavorably with the size of the quantum map. To tackle this issue we employ typicality to assist in finding the control field for such transformation. To demonstrate the method we choose the control task of cooling the fine-structure states of the aluminum monofluoride molecule, at relatively high temperature. As a result high-rotational states are occupied, meaning a high effective Hilbert space. Using quantum typicality, we demonstrate that we can simulate an ensemble of states, enabling a control task addressing simultaneously many states. We employ this method to find a control field for cooling molecules with a large number of internal sates, corresponding to high initial temperatures.

DOI: 10.1103/PhysRevA.107.022603

I. INTRODUCTION

Controlling quantum phenomena has been a primary goal in quantum physics and chemistry. Quantum control theory addresses this topic and has evolved rapidly over the last three decades [1]. One of the aims of quantum control theory is to establish a series of systematic methods to manipulate and control quantum systems. Quantum control theory has been realized in physical chemistry, atomic and molecular physics, and quantum optics. A fundamental issue of quantum control theory is controllability [2]. Controllability concerns the existence of a control solution for a specific task. This problem has practical importance since it closely connects with the universality of quantum computation and the possibility of achieving atomic or molecular state-to-state transformations. In finite-dimensional quantum systems, the controllability criteria can be expressed in terms of the structure and rank of the corresponding Lie groups and Lie algebras [3,4].

The existence of a controllable task does not supply a constructive method allowing one to obtain the control field. For this task, iterative schemes have been developed typically based on constrained optimization [5–11]. The computation complexity of calculating a control solution increases significantly with the dimension of the quantum map and less so with the total Hilbert space size [7].

In our case, the problem is twofold; First, our primary step for each iteration requires solving the time-dependent Schrödinger equation. This has to be done for each participating initial state. The computation complexity scales between $M \times N \log N$ and $M \times N^2$ where N is the size of Hilbert space of our system and M the number of time steps, which in turn scale as $M \propto O(\Delta E \times t)$, where t is the time interval and ΔE the energy range [12].

Second, the number of iterations for solving a unitary control problem and the complexity class of the cooling transformation is estimated to scale between K and $K!$, where K is the size of the transformation [7]. Altogether the control problem is computationally highly complex [13].

This challenge requires establishing methods able to reduce $L < K$, the effective number of states required for optimization. To address this task, we will employ the properties of quantum typicality.

Quantum typicality states that a single quantum state can typically well describe local expectation values of a quantum ensembles. This statement applies to Schrödinger-type dynamics in high-dimensional Hilbert spaces. As a consequence, individual dynamics of expectation values converge to the ensemble's average [14]. We will harness the properties of quantum typicality to calculate the control field by employing random phase wave functions (RPWFs).

The random phase wave function method uses an ensemble of pure states, generating an efficient representation of the mixed state of the entire system. The convergence of the RPWF method becomes faster as the size of the Hilbert space increases. This size significantly increases with the initial system temperature.

There are many ways of cooling particles; one of the most effective is radiative cooling. The basic technique is to locate a closed loop of stimulated excitation and spontaneous emission. The cooling is achieved by entropy removal by spontaneous emission. This technique has been employed to reduce the temperature of translational as well as internal degrees of freedom of atomic and molecular species [15–19].

The present study aims to develop an optimal control algorithm aimed at cooling molecular internal degrees of freedom [16]. This problem is a multistate control task.

*aviv.aroch@mail.huji.ac.il

A possible control objective for cooling could be to concentrate the population on the ground state, as shown in [20]. For high temperatures, this objective is too demanding. We therefore choose a sequential approach that will concentrate the population on a submanifold of lower angular momentum. Once this goal is achieved, we repeat the process with a lower angular momentum restriction. Indirectly the procedure will monotonically increase the purity of the state $\mathcal{P} = \mathrm{Tr}\{\hat{\rho}^2\}$. An alternative control objective is to increase the purity together with additional constraints in the control equation [21]. We choose the first option since for high-entropy states the gradient of purity will be very small.

There is a correlation between increasing purity, lowering entropy, and effective temperature. The effective temperature T_{eff} is defined by a passive Gibbs state which has the same von Neumann entropy [22,23]. This passive state can be related to a thermal Gibbs state with a fixed temperature. In general, one can find a unitary transformation that can transform our system to a passive state with equal entropy. The field of study of cold and ultracold molecules has rapidly grown in the last decade. Cold molecules have an essential role in many active areas in science among tests of fundamental physics, cold chemistry, quantum technologies, and quantum information [16,24–29].

Another crucial consideration in cooling internal degrees of freedom in molecules is enforcing a close transition cycle. Excitation may result in the molecule ending in a different state outside the closed loop after decay; thus, cooling molecules by laser excitation is complicated, and only a few examples exist [29].

We choose optimal control theory to overcome the molecular complexity and enforce closed-loop solutions. Controlled laser fields are employed to remove frequencies that damage the required transition, and the control can steer a quantum system from its initial state to its final one (target state). Optimal control theory (OCT) was created to do this task with maximum fidelity (defined by the user).

OCT is employed for an isolated system to obtain the field leading to the target state. However, this alone cannot result in a colder state (pure state); entropy is invariant under unitary transformation. Therefore cooling requires dissipation that can change the entropy (purity) of our quantum system. In cases with distinct timescale separation between the unitary control and the dissipative step [30], we set an objective for the unitary part which is determined by the dissipation. The unitary dynamics is aimed to shape the system into a state that will be cooled at longer timescales by uncontrolled interaction with the environment. See below (Sec. III A) for a more detailed description of the multistate control.

Assuming that the ultimate target of the process is to reach a pure, single state, any proposed mechanism for the process has to maintain the population of the single-target state while allowing the population of all other states to repopulate selectively. However, as was shown in [31,32], the specific choice of the precooling transformation is a subtle issue. For achieving this step, an ensemble of a single rovibrational state should be created.

Our control objective is to design and enhance the initial preparation; it can be used as a purification method to add molecules that are not resonant with magneto-optical trap [33] transition and thus increase the number density of the initial ensemble.

Specifically, we choose to cool the fine-structure levels of the aluminum monofluoride (AlF) molecule with a large total orbital angular momentum at 30 K, typical of supersonic beams. Spectroscopic measurements and detailed analysis [34] have shown that such a task is feasible using optimal control theory. This molecule belongs to a family of molecules where the vibrational manifold is closed due to a Franck-Condon (FC) coefficient close to one [35,36]. The obstacle in achieving this task is the large initial number of rotational states.

The paper is arranged as follows: Sec. II describes the model in which we implemented our tools. Section III describes the theoretical tools used for achieving control. Section IV presents the results, which are discussed and summarized in the concluding Sec. V.

II. THE MODEL

The model we employ describes the rovibrational structure of the AlF molecule. The state of the systems is defined by the combined density operator of two rovibrationic subspaces:

$$\hat{\rho} = \hat{\rho}_\Sigma \otimes \hat{P}_\Sigma + \hat{\rho}_\Pi \otimes \hat{P}_\Pi + \hat{\rho}_c \otimes \hat{S}_+ + \hat{\rho}_c^* \otimes \hat{S}_-, \quad (1)$$

where $\hat{P}_{\Sigma/\Pi}$ are the projection operators of the ground and excited electronic states, $\hat{S}_{+/-}$ are the electronic raising and lowering operators, $\rho_{\Sigma/\Pi}$ is the density operator for the rovibrational ensemble within the ground and excited electronic states, and $\hat{\rho}_c$ is the density operator of the nuclear coherence between the surfaces. For AlF, we assume an initial temperature of ∼30 K, for which the population of the states occupies up to $J = 11$ (144 sublevels on the ground $^1\Sigma$ state).

The Liouville–von Neumann equation governs the evolution of the system:

$$\frac{d\hat{\rho}}{dt} = -\frac{i}{\hbar}[\hat{H}, \hat{\rho}] + \mathcal{L}_D(\hat{\rho}). \quad (2)$$

The first term is the coherent dynamical part governed by the Hamiltonian, and the second is the dissipative part of the dynamics. This equation represents the dynamics of an open quantum system.

For optical transitions with multiple pulses, there is a distinct three timescale separation between the various processes: (1) the unitary light-induced step occurs on the picosecond timescale, (2) the incoherent decay takes place in tens of nanoseconds, and finally (3) the pulse repetition rate is in the MHz to KHz range.

Each cooling cycle could be separated within this picture into two parts: (1) first, the short-time interaction occurs between the external field and the molecular system. Since this step is unitary, the density operator can be decomposed to energy eigenstates, and each component can be computed in a wave function framework. Then (2) a slow and field-free, spontaneous decay takes place. In this step, the coherences developed between energy eigenstates during the laser-controlled stage are erased.

The Hamiltonian, which governs the unitary part of the dynamics, can be written as

$$\begin{aligned}\hat{H}_t &= \hat{H}_0 + \hat{V}_t,\\ \hat{H}_0 &= \hat{H}_\Sigma \otimes \hat{P}_\Sigma + \hat{H}_\Pi \otimes \hat{P}_\Pi,\end{aligned} \tag{3}$$

where $\hat{H}_{\Sigma/\Pi}$ is the ground and excited rotational Hamiltonian and $\hat{P}_{\Sigma/\Pi}$ the associated projection operators. The interaction of the system with light, assumed to be linearly polarized to the laboratory z axis is described by $\hat{V}_t$:

$$\hat{V}_t = -\hat{\mu}_z \otimes [\hat{S}_+ \varepsilon_z(t) + \hat{S}_- \varepsilon_z(t)^*], \tag{4}$$

where $\hat{\mu}_z$ is the transition dipole moment along the z spatial direction and $\varepsilon_z(t)$ represents the time-dependent field along the same direction.

For mildly cold temperatures ($T_{\text{initial}} \leqslant 30$ K) and high vibrational frequencies, we can assume that the molecules are initially in their ground $v = 0$ state. $\hat{H}_{g/e}$ are the field-free rotational Hamiltonians for the ground vibrational state. Moreover, for the AlF and chemically similar molecules, vibrational excitations in the electronic transition are negligible due to the highly restricting FC factors [37]. The model can thus be restricted to $v = 0$.

Under the Hund's case a, applicable to our case, the rotational states of the model are expanded by the rotational tensor basis [38]

$$|J, \Omega M\rangle = \left[\frac{2J+1}{4\pi}\right]^{\frac{1}{2}} D^J_{M,\Omega}(\phi, \theta, 0), \tag{5}$$

where J is the total molecular angular momentum, and M and Ω are the projections on the spatial (Z) and molecular (z) axes, respectively. Here $D^J_{M\Omega}$ is the rotational tensor. For the ground electronic $^1\Sigma$ state, the projection of the spatial electronic angular momentum on the molecular axis is 0 ($L = S = 0$), therefore $\Omega = 0$, and $J = R$. The rotational Hamiltonian becomes

$$\hat{H}_{\text{rot}} = B_e \hat{\boldsymbol{R}}^2 = B_e \hat{\boldsymbol{J}}^2, \tag{6}$$

where B_e is the rotational constant for the electronic state e and $\boldsymbol{R}$ is the nuclear rotational angular momentum operator, which is equal to $\boldsymbol{R} = \boldsymbol{J} - \boldsymbol{L} - \boldsymbol{S}$, $\boldsymbol{L}$ is the electronic orbital angular momentum, and $\boldsymbol{S}$ is the electronic spin angular momentum.

The $^1\Sigma$ energies are then

$$E(^1\Sigma; J) = B_\Sigma J(J+1), \tag{7}$$

and its corresponding eigenstates can be defined by $|J\Omega M\rangle$ with $\Omega = 0$. In the excited $^1\Pi$ state $\Omega = \pm 1$.

The rotational Hamiltonian for the excited state, $^1\Pi$, is

$$\hat{H}_{\text{rot}}(r) = B_\Pi \hat{\boldsymbol{R}}^2 = B_\Pi (\hat{\boldsymbol{J}} - \hat{\boldsymbol{L}})^2, \tag{8}$$

its energies are

$$E(^1\Pi; J) = B_\Pi [J(J+1) - 1], \tag{9}$$

and the corresponding eigenstates are $|J\Omega M\rangle$ where $\Omega = \pm 1$.

The transitions between the two electronic states $^1\Sigma \rightarrow {}^1\Pi$ are dictated by dipole selection rules ($\Delta J = 0, \pm 1$), denoted as R, Q, and P branches, respectively. The coupling elements can be found by calculating the overlap of any two eigenvectors with the dipole operator,

$$\begin{aligned}&\int D^{J'}_{M'\Omega'}(\theta, \phi, 0) D^1_{0q}(\theta, \phi, 0) D^J_{M\Omega}(\theta, \phi, 0)\, d\Omega\\ &\quad = 8\pi \begin{pmatrix} J & 1 & J' \\ -M & 0 & M' \end{pmatrix} \begin{pmatrix} J & 1 & J' \\ -\Omega & q & \Omega' \end{pmatrix},\end{aligned} \tag{10}$$

where $D^1_{0q}(\theta, \phi, 0)$ corresponds to the transition dipole moment μ. The value of q is determined for a given transition case and is equal to $q = \Omega - \Omega'$.

At thermal equilibrium, the initial state ρ_{eq} is characterized by

$$\hat{\rho}_{eq} = \frac{1}{Z} \sum_j e^{-\beta E^j_\Sigma} |\phi_j\rangle\langle\phi_j|, \tag{11}$$

where $\beta = 1/k_b T$, the sets $|\phi_j\rangle = |J0M\rangle$ and $\{E^j_\Sigma\}$ are the eigenstates and eigenenergies of the ground electronic state, and Z is the partition function.

The dissipating part of the dynamics is generated by the Liovillian superoperator $\mathcal{L}_D$, Eq. (2). Integrating in time leads to the transition map $\Lambda_t = e^{\mathcal{L}_D t}$. Assuming that the timescale between pulses is longer than the spontaneous emission, the transition map $\mathcal{D}$ of the spontaneous emission can be defined. The matrix elements of $\mathcal{D}$ describe the decay from a given excited state energy eigenstate to a given rotational level within the ground-state manifold of states. The elements are calculated employing Fermi's golden rule:

$$\Gamma_{i\rightarrow f} = \frac{2\pi}{\hbar} |\langle f|\mu_z|i\rangle|^2 \rho(\Delta E), \tag{12}$$

where $\langle f|\mu_z|i\rangle$ is the matrix element of the electronic transition dipole between the final and initial states, and $\rho(\Delta E)$ is the density of states of the radiation in the vacuum at the energy gap ΔE. We note hereby that the rotational selection rules in our system dictate narrow band transitions, which means that the density of states is nearly constant and the transition is determined practically by the transition matrix elements.

As implied by the ergodic theorem [39], for a fully connected, ergodic system, under multiple cycles of a given field-driven unitary transformation and subsequent decay, any initial state will coincide finally with the invariant states of the whole transformation. After many excitation-relaxation cycles, the memory of the initial state will be erased. The entire transformation can be described by the following: let $\mathcal{U}$ be the unitary superoperator and $\mathcal{D}$ be dissipative superoperator; then there is a stationary state $\hat{\rho}_{ss}$ that will obey

$$\lim_{n\rightarrow\infty} (\mathcal{U}\mathcal{D})^n \hat{\rho} = \hat{\rho}_{ss}, \tag{13}$$

where $\hat{\rho}$ can be any initial state, and $\mathcal{U}\bullet = \hat{U} \bullet \hat{U}^\dagger$. That is, under a given $\mathcal{U}$ and $\mathcal{D}$, the system will finally evolve from any state into the single stationary $\hat{\rho}_{ss}$. This form is justified when a timescale separation exists between the unitary dynamics and spontaneous emission. In our system the pulse duration is in the sub-ns regime and the dissipation is on the scale of microseconds. In this way we look for a unitary control transformation that under a known dissipator will lead into a purer state [17].

One can obtain the state ρ_{ss} by diagonalization of the full map $\mathcal{UD}$. The first eigenstate corresponds to the stationary state with a unit eigenvalue, while the next eigenvalue indicates the system's convergence rate to steady state.

To associate an effective temperature with the obtained nonthermal state ρ_{ss}, we employ the von Neuman entropy to scale the purity and define the effective temperature. The idea comes from information theory, where the entropy is related to the probability distribution of an ensemble [40]. The entropy is defined as

$$S_{vN} = -tr\{\hat{\rho}\ln\hat{\rho}\} \leqslant -\sum_j P_j \ln P_j, \tag{14}$$

where $\hat{\rho}$ is the system's density matrix, and P_j is the probability to be in the energy eigenstate j. This is the only contribution to the entropy, assuming that quantum coherences do not survive the spontaneous emission incoherent step. Equality will be obtained when the system is diagonalized in the energy domain. It is important to note that entropy is invariant under unitary transformation. Therefore any steady state reached after cooling can be transformed by unitary transformation to a passive state with the same entropy [41]. To define a temperature of any nonthermal state, we associate it with the temperature of a thermal state with the same von Neumann entropy [22].

III. METHODS

A. Optimal control theory (OCT)

Quantum optimal control theory is a branch of coherent control, a quantum-mechanical-based method for controlling dynamical processes. The basic principle is to control quantum interference phenomena typically by shaping the phase of laser pulses [5,6,9,42]. OCT is formulated as an extremum problem and seeks a time-dependent field that minimizes or maximizes the expectation value of an operator in final time. Consider a quantum system in an initial state: $\hat{\rho}_0 = \sum_{k=1}^{K} p_k|\psi_k^0\rangle\langle\psi_k^0|$, where the set $\{\psi_k^0\}$ is energy eigenstates of the system, and here K is the size of a subsystem within the full Hilbert space of size N. In our case, the control will seek a field that maximizes the expectation value of the operator $\hat{O}$ at final time T:

$$\mathcal{J}_{\max}(\varepsilon_z) \equiv \mathrm{tr}\{\hat{O}\hat{\rho}_T\} = \sum_{k=1}^{K} p_k\langle\psi_k(T)|\hat{O}|\psi_k(T)\rangle, \tag{15}$$

where $\psi_k(T) = \hat{U}(T)\psi_k^0$ describes the state that results from the interaction of the system with the field $\varepsilon_z(t)$ at the final time T.

The objective operator $\hat{O}$ chosen is a projection operator, defined as

$$\hat{O} = \hat{P}_\Sigma \otimes \sum_{j}^{J_\Sigma=10} |\psi_j\rangle\langle\psi_j| + \hat{P}_\Pi \otimes \sum_{l}^{J_\Pi=9} |\psi_l\rangle\langle\psi_l|, \tag{16}$$

where $\psi_{j/l}$ is a set of eigenvectors in of the $^1\Sigma$ and $^1\Pi$ electronic states, respectively. For an ensemble that corresponds to $T = 30$ K, 99.9% of the population resides in states up to $J = 11$. To ensure a close loop of the cycle that starts off with $J_{\max} = 11$, we choose for the transition a cutoff angular momentum as $J_\Sigma = 10$ and $J_\Pi = 9$. This ensures that the population will concentrate at lower angular momentum without leakage to higher states. To account for possible transitions to a higher state the simulation includes all the rotational states up to $J = 12$.

The quantum dynamics is enforced by adding an additional cost term to the functional, according to the Lagrange-multiplier method:

$$\mathcal{J}_{\mathrm{con}} = \sum_{k=1}^{K} -2\mathrm{Re}\int_0^T \langle\chi_k(t)|\frac{d}{dt} + i\hat{H}(t)|\psi_k(t)\rangle dt, \tag{17}$$

where $\{\langle\chi_k(t)|\}$ are the set of time-dependent Lagrange function multipliers. To regularize the solution with a limitation over the field intensity another penalty term to the functional is added [43]:

$$\mathcal{J}_{\mathrm{penal}}(\varepsilon_z) = -\int_0^T \alpha\varepsilon_z^2(t)\,dt, \tag{18}$$

where α is a penalty parameter to the functional. It penalizes the object of the maximization for using high-intensity fields.

The overall functional is

$$\mathcal{J} = \mathcal{J}_{\max} + \mathcal{J}_{\mathrm{penal}} + \mathcal{J}_{\mathrm{con}}. \tag{19}$$

The maximization of the generalized objective $\mathcal{J}$ is the control task. Functional derivatives with respect to the various functional elements are then taken resulting in the following system of equations

Each of the set of the $|\chi_k(t)\rangle$ Lagrange function multipliers will obey a time-reversed Schrödinger equation

$$\frac{d\langle\chi_k(t)|}{dt} = i\langle\chi_k(t)|\hat{H}(t), \tag{20}$$

and each of the states in our system follows the Schrödinger equation

$$\frac{d|\psi_k(t)\rangle}{dt} = i\hat{H}(t)|\psi_k(t)\rangle \tag{21}$$

with the boundary conditions $|\chi_k(T)\rangle = \hat{O}|\psi_k(T)\rangle$ [44].

The Krotov iterative method is applied to obtain a monotonic growth of of the generalized objective $\mathcal{J}$ at each iteration with the updated field so that

$$\varepsilon_z^{n+1}(t) = \varepsilon_z^n(t) - \frac{1}{\alpha}\sum_{k=1}^{K}\mathrm{Im}\langle\chi_k^n(t)|\hat{\mu_z}|\psi_k^{n+1}(t)\rangle, \tag{22}$$

where $\varepsilon_z^n(t)$ denote to the field after the nth iteration.

Note that the scheme of Eqs. (20)–(22) is somewhat similar to the simultaneous optimization scheme that is required for unitary transformations and quantum gates [9,45–47]. However, for cooling, each cycle at the final transformation erases the relative quantum phases between the various set of initial states. This leaves the resulting fitness measurement at the level of classical transition probability between the initial and final state and removes the need to evaluate quantum phases. One can compare Eq. (22) to Eq. (47) in Ref. [7].

B. Quantum typicality

Typicality describes a property of a system where a typical state can present an assembly of similar states. This set of

states should have a narrow distribution of some feature (e.g., drawn according to the same distribution, sharing the same energy, etc.) and therefore yield a very limited distribution of expectation values. The typical state will fit the expectation value of the complete set of states.

Quantum typicality was first noted by Schrödinger and von Neumann when they were trying to incorporate statistical mechanics with quantum mechanics. They inferred that the wave function of a complex system can have statistical properties [48].

In their approach, when discussing thermalization in isolated quantum systems, one should focus on physical observables instead of wave functions or density matrices describing the entire system. This approach is similar to eigenvalue thermaliziation hypothesis (ETH), in which the focus is put on macroscopic observables and "typical" configuration. ETH implies that the expectation values of local observables and their fluctuations in isolated quantum systems relax to (nearly) time-independent values that can be described using traditional statistical mechanics ensembles. This has been verified in several quantum lattice systems and, according to ETH, should occur in generic many-body quantum systems. ETH states that the eigenstates of generic quantum Hamiltonians are "typical" in the sense that the statistical properties of physical observables are the same as those predicted by the microcanonical ensemble. [49,50]

Our quantum typicality refers to an idea that anticipates that almost all quantum systems will have similar dynamical properties [51].

C. Random phase states

Controlling the dynamics of an extensive system is practically impossible when the system becomes large and complex. Formally our control strategy requires all the thermally populated Σ states in Eqs. (15) and (17).

We know from Ref. [52] that sampling quantum states at random can be seen to be induced by the sampling of unitaries at random. Sampling a set of unitaries, which are bounded, means we sample a set of actions we can apply to our state, which is global.

We will now sample using a random state, as follows:

$$|\psi(\vec{\theta})\rangle = \frac{1}{\sqrt{K}} \sum_{j}^{K} e^{i\theta_j} |\phi_j\rangle, \tag{23}$$

where $\vec{\theta} = (\theta_1, \theta_2, \ldots, \theta_K)$ is a vector of random phases, K is the size of the relevant states for the transformation, and $|\phi_j\rangle$ is a basis set of the full system [53–56]. Employing a random set defined by different $\vec{\theta}$ we can resolve the identity

$$\hat{I} = \lim_{L\to\infty} \frac{1}{L} \sum_{l=1}^{L} |\psi(\vec{\theta}_l)\rangle\langle\psi(\vec{\theta}_l)|. \tag{24}$$

Employing now L random states to sample the control and relying on quantum typicality we expect $L < K < N$.

IV. RESULTS

Our primary goal in this study is to develop a method to enable control systems with large Hilbert space. The objective of the present model was to cool by increasing the system's purity at the final steady state after multiple cycles using the OCT algorithm. It is important to note that this objective is a multistate problem. We have shown that such a task is possible for smaller systems [17], but the main drawback is the computation scaling of the problem with the system's size.

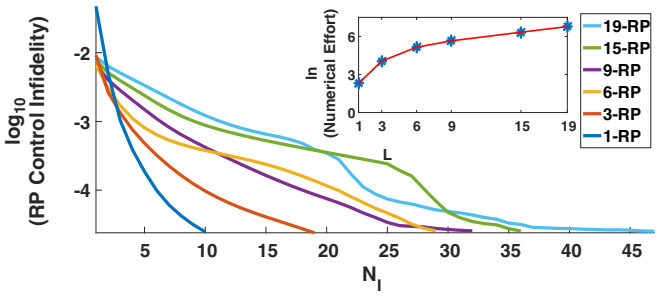

FIG. 1. The controlled infidelity $\mathcal{F}$ (log scale), of different number random phase sampling, as a function of the number of iterations required to converge the control ($\approx 99\%$ at the target state). The number of RPWF L is assigned by different colors in the legend. The number of states of each model influences the number of iterations, increasing monotonically. Inset: The numerical effort (log scale) as a function of the number of random phase states. The numerical effort is a function of Hilbert space size times the number of iterations, showing a polynomial scaling.

Assuming that the target of the process is to reach a colder state, any proposed mechanism for the process has to maintain the population of the target state while allowing the population of all other states to repopulate selectively. After many excitation-relaxation cycles, the memory of the initial state will be erased, and the obtained transformation will be of which mentioned in Eq. (13). In this model, rotational cooling of AlF (Sec. II), we defined the cost function $\mathcal{J}_{\max}$ to populate states which through spontaneous emission will populate lower J values and penalize increase in J values; see above, Eq. (16). To control this type of system we have created several realizations for an increasing number of random states L to control the transformation. We want to check the following:

(1) Can the total transformation be faithfully represented?

(2) If it does, how many states L are required to converge the entire system's population, and in turn the cooling transformation [see Eq. (16)], sufficiently?

A. Approximated optimal control under RPWF

The optimal field should depend on the random phases of the initial state of the system. This behavior has been observed for state-to-state quantum objectives when the Hilbert space size increased [57]. The idea of using RPWF is the hope that the effect of different phases will be averaged out with the increase of L.

Figure 1 displays the infidelity $\mathcal{F} = 1 - \mathcal{J}_{\max}$ of the control for systems with a different number of random states L as a function of the number of iterations. For good comparability, each control with L number of RPWF was initiated with the same guess field.

We studied a controlled scheme employing a single field polarized on the Z axis. The initial population distributed among different random states corresponds to a system with $J = 11$ so that the full Hilbert space is of the size $N = 430$. The target was to move the population to all the states in the Hilbert space, up to an excited state at $J \leqslant 10$ and eliminate any transitions to higher J states that open decay channels to even higher states. The control field was taken as the one that manipulates the system towards the target state with a fitness of $\mathcal{F} = 99\%$. However, this fidelity fits only the contracted space and is therefore an approximation; later we will show that the same field acting on the full space system results in lower fidelity. Thus, some population is leaking outside the desired closed loop of cooling. To ensure that the control end up in cooling we demand high fidelity for this approximated solution.

In Fig. 1 we observe that the number of random phase states L employed in the control simulation influences the number of iteration. The trend reflects the increase complexity of multistate control. As the number of states increases, the control requires more destructive and constructive interference. Finding the control becomes harder in terms of the number of iterations. In the inset we show how the numerical effort increases subexponentially, i.e., polynomially. The effort is defined by the following: $N_{\text{Effort}} = \log(N_I \times L_{RP})$ [7,44] where L_{RP} is the number of random phase states used in this model and N_I states the number of iterations needed for the control algorithm to converge to the predetermined threshold.

We noted that one can employ control fields obtained from a small L as an initial guess to a larger L, the so-called the pilot fields method [57]. Our attempt to use the method enabled to filter out the frequency spectrum. However, beyond that, the pilot guess field did not significantly improve the convergence. This is probably due to the fact that this step is not the rate-determining step of the problem (see below).

We now move to a more careful look at the relation between the obtained control fields for a different number of random phase states. Figure 2 displays the frequency and time comparison between for fields with different number of random phase states. The frequencies are computed within the rotating frame and are presented in the dressed state picture with respect to the resonance frequency, which lies in the visible regime. Examining the optimized control fields for each of the different random phase cases shows the following:

(1) When comparing to the initial guess, chosen to be ∼500 ps in length, additional frequencies are obtained. In addition a shift in the low frequencies is observed.

(2) All the control fields show 99% identical spectrum in the frequency domain up to ∼3 cm^{-1}. Deviations are observed in the high-frequency range. The different frequencies result from further interference resulting from adding random phase states and constitute the fine-tuning part of the pulse. This fine tuning is the part responsible for high fidelity from 90% to 99%. To verify the importance of the frequency components we applied the resulted field, filtering out high frequencies from it. The obtained fitness was 90.5%, and the pulse was found to lead to heating (see below for technical details)

(3) As we have seen, the solution for the different number random phase is distinct in the high-frequency range (when asking for high fidelity); as a result, the idea of using a seed pulse for accelerating the iteration process had only marginal effect.

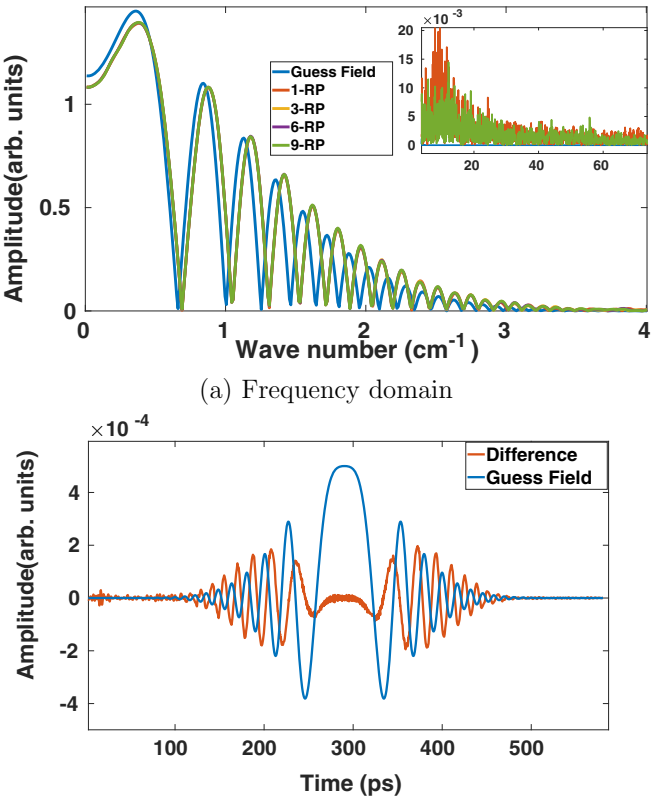

(a) Frequency domain

(b) Time domain

FIG. 2. Field analysis in the frequency (up) time of time (down) domains. In both panels, the initial Guess field is in blue. (Top) The optimal control field for $L = 1, 3, 6, 9$ random phase optimizations up to the frequency of ∼3 cm^{-1} (superimposed on each other). The insert shows the high-frequency range of $L = 1$ compared to $L = 9$ where differences in the optimal field can be observed. (Bottom) Time domain: (blue) the initial guess field and (red) the difference between the guess and optimal field for $L = 3$. One can notice the addition of higher frequencies.

B. Application of the full map transformation

The fidelity that was achieved in Fig. 1 measures the obtained quality of the transformation for the truncated set of random phase states. This by itself does not imply a comparable fidelity for the actual transformation of the thermal system. The main assessment of this work is that high fidelity for a large enough set of random phase states will lead eventually to a better description of the optimal field for the whole thermal system.

To check the quality of the transition we used the field from the controlled scheme and computed explicitly the exact dynamics of the entire system to compute the full system infidelity $\mathcal{F}_{\text{map}}$ defined at the same as $\mathcal{F}$, now for the full thermal ensemble as the initial state. Figure 3 shows the infidelity of the entire system as a function of the number of random phase states L, and a monotonic growth of fidelity corresponding to the number L of random states can be seen.

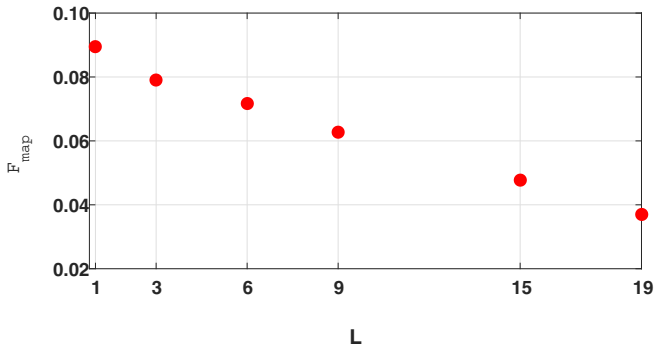

FIG. 3. The infidelity as a function of the number of random phase base functions L. The full map infidelity is calculated from the fixed point of the full transformation (13) employing the control field from the random phase sampling.

The transformation fidelity of the full system is, as expected, smaller than the one obtained from the control calculated from a finite set of random phase states. This is, in fact, the actual measure for the quality of the random phase approximation. To find the number of random states which lead to convergence, we extrapolate our results, taking infidelity as a measure.

In Fig. 4 we have fitted our calculated points to an exponential curve. Defining an acceptable threshold we get the number of sampling states L required to converge the full system of dimension K.

The marked point is a good guess as to the complexity of the transformation corresponding to an effective transformation size of $L = 44$, which corresponds to the fidelity of the control sequence (0.99). If a different target fidelity was chosen, the effective size will change. Nevertheless the fidelity cannot exceed the fidelity set by the control. The computation effort for this sampling space is very high. The effective transformation size is still much smaller than the dimension of the full transformation.

A concrete measure for cooling in our context is the change in the normalized entropy. Employing Eq. (14) we define the normalized entropy decrease:

$$\Delta_S^{\text{eff}} = \frac{S_{\text{FS}}^{\text{RP}} - S_{\text{initial}}^{J=11}}{S_{\text{Th}}^{J=10} - S_{\text{initial}}^{J=11}}, \tag{25}$$

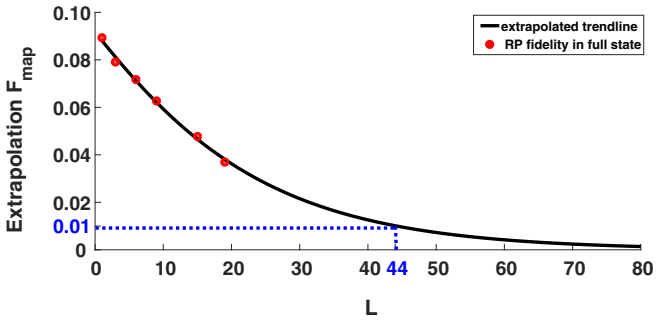

FIG. 4. Fitting the infidelity of the full transformation as a function of the number of random phase states (red dots). Extrapolating (black curve) to high fidelity allows for estimating the effective size of the cooling transformation (44,0.01).

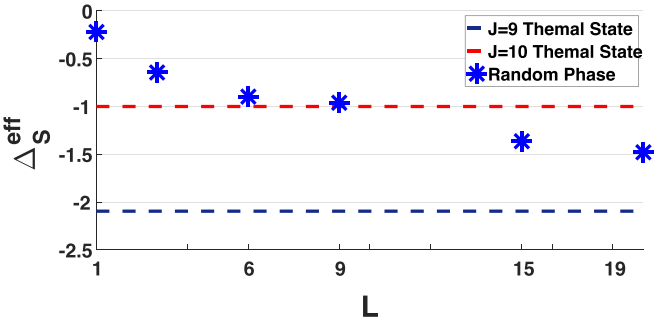

FIG. 5. The monotonic decrease of normalized entropy, Eq. (25) with L, for the complete transformation obtained by each random phase model (blue stars). The entropy value of the thermal state at $J = 10$ is marked by a red line and for $J = 9$ by a blue line. The objective of the full transformation was to deplete $J = 11$, but it is clear that for the 19-RP model we accomplished an even colder state ($T = \sim 30$ K).

where S_{FS}^{RP} is the entropy of the steady state of the full system obtained from the control sequence and diagonalization of $(\mathcal{UD})$ [see Eq. (13)], $S_{\text{initial}}^{J=11}$ is the thermal entropy of the initial state ($J = 11$), and $S_{Th}^{J=10}$ is the entropy of a thermal state at $J = 10$, the original target of the cooling transformation. Thus, Δ_S^{eff} measures the relative distance between the expected and actual cooling achieved in the process. The normalization is with respect to the thermal entropy difference between $J = 11$ and $J = 10$.

Figure 5 shows the effective change in entropy vs L, the number of RPWF. A monotonic decrease of the effective entropy is a clear indication for cooling.

An ensemble of typical states should have a small standard deviation with respect to a local observable. This is confirmed by Fig. 6, displaying the standard deviation of the target infidelity when the size of the sample increases. Each sample is composed of independent random realizations with different L random wave functions. We expect convergence as $\frac{1}{\sqrt{n}}$, where n is the sample size. The fidelity obtained for the full system for each realization was used to calculate of the standard deviation, defined by $\text{STD} = \frac{\sqrt{\sum_j^n (\langle \hat{O} \rangle_j - \langle \hat{O}_{av} \rangle^2}}{|\langle \hat{O} \rangle_{av}|}$,

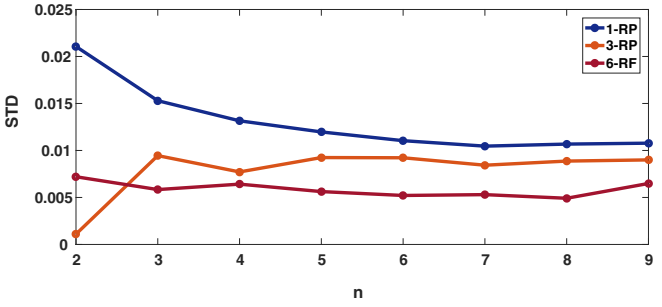

FIG. 6. The standard deviation (STD) of the infidelity of the full Hilbert space as a function of the number of samples (n). The blue curve is data obtained by optimizing a single random phase model. The orange curve was obtained for simultaneous transformation for 3-RP sampling. The red curve was obtained for simultaneous transformation for 6-RP sampling.

where $< \hat{O} >_{av} = \sum_j^n \langle \hat{O} \rangle_j$. In Fig. 6 we show how the STD behaves in different schemes. The samples describe different realizations, where the initial states were created randomly. We have used the control fields of these realizations for transformation on the full system.

The standard deviation is quite small for the random phase wave function sampling. As expected, when random transformation L is larger (3-RP and 6-RP) the STD decreases demonstrating self-averaging.

V. CONCLUSIONS

Laser cooling of the internal degrees of freedom of a molecule is a difficult task due to the large occupied Hilbert space. In cooling molecules one cannot ignore rotation [28,58–61]. A shaped pulse generates a population transformation accompanied by spontaneous emission. We optimize the population transition $\mathcal{U}$ such as after many cooling cycles the target state is colder than the initial one. This quantum control task is a multistate transformation that scales unfavorable with the size of the transformation. We have utilized quantum typicality to assist in optimizing the cooling map. The transformation is calculated with a reduced set of random phase wave functions. We show convergence (of infidelity) to the desired cooling transformation. The method provides a control solution for multistate tasks that were never been achieved previously, to the best of our knowledge. The optimal control field is not unique. It has already been stated that the top of the optimization mountain is flat [62]. It is important to note that the number of random phase states needed to converge in OC method are proportional to size of the total transformation and the target chosen.

Moreover, we have found that the quality of the transformation is sensitive to high-frequency components. We are currently exploring the effect of noise and other inaccuracies on control problems in general.

Finally, we have shown that this method can be utilized to model cooling of internal degrees of freedom of molecules. It is anticipated that a series of such transformations, which are independent, can cool the rotation toward its ground rotational state.

ACKNOWLEDGMENTS

We thank Gerard Meijer for his helpful discussions. This study was supported by the Israel Academy of Sciences and Humanities and by the Israel Science Foundation (Grants No. 510/17 and 526/21).

[1] S. J. Glaser, U. Boscain, T. Calarco, C. P. Koch, W. Köckenberger, R. Kosloff, I. Kuprov, B. Luy, S. Schirmer, T. Schulte-Herbrüggen *et al.*, Training Schrödinger's cat: Quantum optimal control, Eur. Phys. J. D **69**, 279 (2015).

[2] G. M. Huang, T. J. Tarn, and J. W. Clark, On the controllability of quantum-mechanical systems, J. Math. Phys. **24**, 2608 (1983).

[3] F. Albertini and D. D'Alessandro, Notions of controllability for bilinear multilevel quantum systems, IEEE Trans. Autom. Control **48**, 1399 (2003).

[4] V. Ramakrishna, M. V. Salapaka, M. Dahleh, H. Rabitz, and A. Peirce, Controllability of molecular systems, Phys. Rev. A **51**, 960 (1995).

[5] A. P. Peirce, M. A. Dahleh, and H. Rabitz, Optimal control of quantum-mechanical systems: Existence, numerical approximation, and applications, Phys. Rev. A **37**, 4950 (1988).

[6] R. Kosloff, S. A. Rice, P. Gaspard, S. Tersigni, and D. Tannor, Wavepacket dancing: Achieving chemical selectivity by shaping light pulses, Chem. Phys. **139**, 201 (1989).

[7] J. P. Palao and R. Kosloff, Optimal control theory for unitary transformations, Phys. Rev. A **68**, 062308 (2003).

[8] I. Serban, J. Werschnik, and E. K. U. Gross, Optimal control of time-dependent targets, Phys. Rev. A **71**, 053810 (2005).

[9] J. Werschnik, and E. K. U. Gross, Quantum optimal control theory, J. Phys. B: At. Mol. Opt. Phys. **40**, R175 (2007).

[10] R. Eitan, M. Mundt, and D. J. Tannor, Optimal control with accelerated convergence: Combining the Krotov and quasi-Newton methods, Phys. Rev. A **83**, 053426 (2011).

[11] D. M. Reich, M. Ndong, and C. P. Koch, Monotonically convergent optimization in quantum control using Krotov's method, J. Chem. Phys. **136**, 104103 (2012).

[12] R. Kosloff, Time-dependent quantum-mechanical methods for molecular dynamics, J. Phys. Chem. **92**, 2087 (1988).

[13] S. Arora and B. Barak, *Computational Complexity: A Modern Approach* (Cambridge University Press, Cambridge, 2009).

[14] C. Bartsch and J. Gemmer, Dynamical Typicality of Quantum Expectation Values, Phys. Rev. Lett. **102**, 110403 (2009).

[15] E. S. Shuman, J. F. Barry, and D. DeMille, Laser cooling of a diatomic molecule, Nature (London) **467**, 820 (2010).

[16] M. R. Tarbutt, Laser cooling of molecules, Contemporary Phys. **59**, 356 (2018).

[17] A. Aroch, S. Kallush, and R. Kosloff, Optimizing the multicycle subrotational internal cooling of diatomic molecules, Phys. Rev. A **97**, 053405 (2018).

[18] W. M. Itano, J. C. Bergquist, J. J. Bollinger, and D. J. Wineland, Cooling methods in ion traps, Phys. Scr. **1995**, 106 (1995).

[19] M. Zeppenfeld, B. G. Englert, R. Glöckner, A. Prehn, M. Mielenz, C. Sommer, L. D. van Buuren, M. Motsch, and G. Rempe, Sisyphus cooling of electrically trapped polyatomic molecules, Nature (London) **491**, 570 (2012).

[20] A. Bartana, R. Kosloff, and D. J. Tannor, Laser cooling of internal degrees of freedom. II, J. Chem. Phys. **106**, 1435 (1997).

[21] C. P. Koch, Controlling open quantum systems: Tools, achievements, and limitations, J. Phys.: Condens. Matter **28**, 213001 (2016).

[22] R. Uzdin and S. Rahav, Global Passivity in Microscopic Thermodynamics, Phys. Rev. X **8**, 021064 (2018).

[23] S. Kallush, A. Aroch, and R. Kosloff, Quantifying the unitary generation of coherence from thermal quantum systems, Entropy **21**, 810 (2019).

[24] R. Krems, B. Friedrich, and W. C. Stwalley, *Cold Molecules: Theory, Experiment, Applications* (CRC Press, Boca Raton, FL, 2009).

[25] J. L. Carini, S. Kallush, R. Kosloff, and P. L. Gould, Enhancement of Ultracold Molecule Formation Using Shaped Nanosecond Frequency Chirps, Phys. Rev. Lett. **115**, 173003 (2015).

[26] S. Kallush and R. Kosloff, Unitary photoassociation: One-step production of ground-state bound molecules, Phys. Rev. A **77**, 023421 (2008).

[27] M. Yeo, M. T. Hummon, A. L. Collopy, B. Yan, B. Hemmerling, E. Chae, J. M. Doyle, and J. Ye, Rotational State Microwave Mixing for Laser Cooling of Complex Diatomic Molecules, Phys. Rev. Lett. **114**, 223003 (2015).

[28] C.-Y. Lien, C. M. Seck, Y.-W. Lin, J. H. Nguyen, D. A. Tabor, and B. C. Odom, Broadband optical cooling of molecular rotors from room temperature to the ground state, Nat. Commun. **5**, 4783 (2014).

[29] N. Fitch and M. Tarbutt, Laser-cooled molecules, Adv. At. Mol. Opt. Phys. **70**, 157 (2021).

[30] S. E. Sklarz, D. J. Tannor, and N. Khaneja, Optimal control of quantum dissipative dynamics: Analytic solution for cooling the three-level λ system, Phys. Rev. A **69**, 053408 (2004).

[31] Y. Maday and G. Turinici, New formulations of monotonically convergent quantum control algorithms, J. Chem. Phys. **118**, 8191 (2003).

[32] D. M. Reich and C. P. Koch, Cooling molecular vibrations with shaped laser pulses: Optimal control theory exploiting the timescale separation between coherent excitation and spontaneous emission, New J. Phys. **15**, 125028 (2013).

[33] J. Barry, D. McCarron, E. Norrgard, M. Steinecker, and D. DeMille, Magneto-optical trapping of a diatomic molecule, Nature (London) **512**, 286 (2014).

[34] S. Truppe, S. Marx, S. Kray, M. Doppelbauer, S. Hofsaess, H. C. Schewe, B. Sartakov, and G. Meijer, Spectroscopy, buffer gas cooling and radiation pressure slowing of alf molecules, Bull. Am. Phys. Soc. **64**, (2019).

[35] M. V. Ivanov, F. H. Bangerter, and A. I. Krylov, Towards a rational design of laser-coolable molecules: Insights from equation-of-motion coupled-cluster calculations, Phys. Chem. Chem. Phys. **21**, 19447 (2019).

[36] M. V. Ivanov, F. H. Bangerter, P. Wójcik, and A. I. Krylov, Toward ultracold organic chemistry: Prospects of laser cooling large organic molecules, J. Phys. Chem. Lett. **11**, 6670 (2020).

[37] S. Truppe, S. Marx, S. Kray, M. Doppelbauer, S. Hofsäss, H. C. Schewe, N. Walter, J. Pérez-Ríos, B. G. Sartakov, and G. Meijer, Spectroscopic characterization of aluminum monofluoride with relevance to laser cooling and trapping, Phys. Rev. A **100**, 052513 (2019).

[38] R. N. Zare, *Angular Momentum* (Wiley, New York, 1988).

[39] T. Brixner, G. Krampert, T. Pfeifer, R. Selle, G. Gerber, M. Wollenhaupt, O. Graefe, C. Horn, D. Liese, and T. Baumert, Quantum Control by Ultrafast Polarization Shaping, Phys. Rev. Lett. **92**, 208301 (2004).

[40] J. Von Neumann, *Mathematical Foundations of Quantum Mechanics* (Princeton University Press, Princeton, 2018).

[41] A. Lenard, Thermodynamical proof of the Gibbs formula for elementary quantum systems, J. Stat. Phys. **19**, 575 (1978).

[42] D. J. Tannor, *Introduction to Quantum Mechanics: A Time-Dependent Perspective* (ACS Publications, University Science Books, Sausalito, Calif., 2007).

[43] I. Degani, A. Zanna, L. SÆlen, and R. Nepstad, Quantum control with piecewise constant control functions, SIAM J. Sci. Comput. **31**, 3566 (2009).

[44] J. P. Palao and R. Kosloff, Quantum Computing by an Optimal Control Algorithm for Unitary Transformations, Phys. Rev. Lett. **89**, 188301 (2002).

[45] C. P. Koch, U. Boscain, T. Calarco, G. Dirr, S. Filipp, S. J. Glaser, R. Kosloff, S. Montangero, T. Schulte-Herbrüggen, D. Sugny *et al.*, Quantum optimal control in quantum technologies. Strategic report on current status, visions and goals for research in Europe, EPJ Quantum Tech. **9**, 19 (2022).

[46] J. Dominy and H. Rabitz, Exploring families of quantum controls for generating unitary transformations, J. Phys. A: Math. Theor. **41**, 205305 (2008).

[47] C. M. Tesch and R. de Vivie-Riedle, Quantum Computation with Vibrationally Excited Molecules, Phys. Rev. Lett. **89**, 157901 (2002).

[48] J. von Neumann, Proof of the ergodic theorem and the H-theorem in quantum mechanics, Eur. Phys. J. H **35**, 201 (2010).

[49] M. Rigol, V. Dunjko, and M. Olshanii, Thermalization and its mechanism for generic isolated quantum systems, Nature (London) **452**, 854 (2008).

[50] L. D'Alessio, Y. Kafri, A. Polkovnikov, and M. Rigol, From quantum chaos and eigenstate thermalization to statistical mechanics and thermodynamics, Adv. Phys. **65**, 239 (2016).

[51] P. Reimann, Typicality for Generalized Microcanonical Ensembles, Phys. Rev. Lett. **99**, 160404 (2007).

[52] P. F. Romero, Equilibration and typicality in quantum processes, Ph.D. thesis, Monash University, Melbourne (2020).

[53] M. Nest and R. Kosloff, Quantum dynamical treatment of inelastic scattering of atoms at a surface at finite temperature: The random phase thermal wave function approach, J. Chem. Phys. **127**, 134711 (2007).

[54] S. Kallush and S. Fleischer, Orientation dynamics of asymmetric rotors using random phase wave functions, Phys. Rev. A **91**, 063420 (2015).

[55] S. Amaran, R. Kosloff, M. Tomza, W. Skomorowski, F. Pawłowski, R. Moszynski, L. Rybak, L. Levin, Z. Amitay, J. M. Berglund *et al.*, Femtosecond two-photon photoassociation of hot magnesium atoms: A quantum dynamical study using thermal random phase wavefunctions, J. Chem. Phys. **139**, 164124 (2013).

[56] B. Ezra, R. Kosloff, and S. Kallush, Simulating photodissociation in strong field by the random phase thermal wavefunction approach, arXiv:2110.12458.

[57] S. Kallush and R. Kosloff, Scaling the robustness of the solutions for quantum controllable problems, Phys. Rev. A **83**, 063412 (2011).

[58] I. S. Vogelius, L. B. Madsen, and M. Drewsen, Rotational cooling of heteronuclear molecular ions with $^1\Sigma$, $^2\Sigma$, $^3\Sigma$, and $^2\Pi$ electronic ground states, Phys. Rev. A **70**, 053412 (2004).

[59] I. Manai, R. Horchani, H. Lignier, P. Pillet, D. Comparat, A. Fioretti, and M. Allegrini, Rovibrational Cooling of Molecules by Optical Pumping, Phys. Rev. Lett. **109**, 183001 (2012).

[60] M. Hamamda, P. Pillet, H. Lignier, and D. Comparat, Ro-vibrational cooling of molecules and prospects, J. Phys. B: At. Mol. Opt. Phys. **48**, 182001 (2015).

[61] C. P. Koch, M. Lemeshko, and D. Sugny, Quantum control of molecular rotation, Rev. Mod. Phys. **91**, 035005 (2019).

[62] K. W. Moore and H. Rabitz, Exploring constrained quantum control landscapes, J. Chem. Phys. **137**, 134113 (2012).